



Precise control of squeezing angle to generate 11 dB entangled state

WENHUI ZHANG,¹ NANJING JIAO,¹ RUIXIN LI,¹ LONG TIAN,^{1,2}
YAJUN WANG,^{1,2,3}  AND YAOHUI ZHENG^{1,2,4} 

¹State Key Laboratory of Quantum Optics and Quantum Optics Devices, Institute of Opto-Electronics, Shanxi University, Taiyuan, 030006, China

²Collaborative Innovation Center of Extreme Optics, Shanxi University, Taiyuan 030006, China

³YJWangsxu@sxu.edu.cn

⁴yhzheng@sxu.edu.cn

Abstract: The strength of the quantum correlations of a continuous-variable entangled state is determined by several relative phases in the preparation, transmission, and detection processes of entangled states. In this paper, we report the first experimental and theoretical demonstrations of the precision of relative phases associated with the strength of quadrature correlations. Based on the interrelations of the relative phases, three precisely phase-locking methodologies are established: ultralow RAM control loops for the lengths and relative phases stabilization of the DOPAs, difference DC locking for the relative phase between the two squeezed beams, and DC-AC joint locking for the relative phases in BHDs. The phase-locking loops ensure the total phase noise to be $9.7 \pm 0.32 / 11.1 \pm 0.36$ mrad. Finally, all the relative phase deviations are controlled to be in the range of -35 to 35 mrad, which enhances the correlations of the amplitude and phase quadratures to -11.1 and -11.3 dB. The entanglement also exhibits a broadband squeezing bandwidth up to 100 MHz. This paves a valuable resource for experimental realization and applications in quantum information and precision measurement.

© 2021 Optical Society of America under the terms of the [OSA Open Access Publishing Agreement](#)

1. Introduction

Continuous variables (CV) quantum entanglement has been widely approved to be a valuable resource in quantum information networks [1–5], quantum computation [6,7], quantum communication [8–14], and quantum precision measurement [15–19]. In these applications, a strong entangled state has been proposed or applied to enhance the performance of the quantum protocols. For example, with -10 dB quantum correlations for the amplitude and phase quadratures, the secure distance of CV quantum key distribution (QKD) can be increased from 190 km (with -3.5 dB two-mode squeezing in the experiment) to 320 km under an excess noise of 0.1 and a modulation of 100 shot-noise units (SNU) [8]; the fidelity of quantum state transmission with quantum teleportation can be promoted from 0.7 (-5.2 dB squeezing) to 0.87 [11]; the non-classical sensitivity of simultaneous measurement of two non-commuting observables in quantum-dense metrology (QDM) can be improved from 6 dB (-7 dB squeezing) to 10 dB [16,20]; the signal-to-noise ratio (SNR) in multiplexing quantum communication can be improved from 7.8 dB (-8 dB squeezing) to 10 dB beyond the shot noise limit (SNL) [12].

Although the need for strong quantum correlations is enormous, it is a complex and tough task to implement an entanglement of more than 10 dB. To achieve the ultimate goal, squeezing factors, the balance of the beam splitter, channel losses, and multiple relative phases in the generation and detection processes of the entangled state must be globally considered. The first three influence factors had been detailly analyzed in an unbiased entangled state preparation with two single-resonant optical parametric amplifiers (OPAs) [21]. However, the multiple relative phases being associated with the squeezing angles are more critical for establishing a more robust entangled state.

Recently, the maximum quantum correlations had been fabricated with the optical parametric oscillator (OPO) [22] or OPA [21] technology. In preparation of the entangled state, two single-mode squeezed states are coupled on a 50/50 beam splitter (BS), which are also accompanied by at least five electronic servo control loops of the relative phases: the signal and pump beam of the OPO or OPA Φ_1 (or Φ_2), the two squeezed beams on the 50/50 BS φ_S , and the entangled beam and local oscillator φ_A (φ_B) in the balanced homodyne detection (BHD). For all of the relative phases, arbitrary deviation from the ideal phase angle will weaken the quantum correlations as well as introduce an asymmetric noise variance for the two quadrature components [21,23]. Moreover, the impact of phase angle deviation becomes acute as the optical loss being reduced to produce an entangled state of more than 10 dB. Currently, entangled quantum correlations have been experimentally or theoretically demonstrated without considering the influence and interrelations of phase angles. To achieve the requirements for stronger entangled states preparation, the precise and stable control of the phase angles is an essential prerequisite. Stable control of the squeezing angle was already feasible and had been demonstrated by using a coherent control technology with the OPO [24,25] or by reducing the residual amplitude modulation (RAM) [26,27] downstream the phase modulator before and after the OPA [28].

This paper theoretically and experimentally demonstrates the associations between the relative phases and quadrature correlations in the OPA process for the first time. By designing three phase-locking methodologies, the interrelations between the relative phases are destroyed and can be individually controlled to high precision, i.e., in the range of -35 to 35 mrad. This paves a way to experimental realization for the -11.1 and -11.3 dB correlations of the amplitude and phase quadratures, and its squeezing bandwidth can be up to 100 MHz.

2. Theoretical analysis for the interrelations of the phase angles

The entanglement [20,22] can be prepared by mixing two amplitude squeezed states \hat{S}_1 and \hat{S}_2 with relative phase $\varphi_S = \frac{\pi}{2}$ on a 50/50 beam splitter (BS), which outputs are two entangled modes A (\hat{a}) and B (\hat{b})

$$\hat{a} = \sqrt{\frac{1}{2}}\hat{S}_1 + \sqrt{\frac{1}{2}}\hat{S}_2e^{i\varphi_S}, \hat{b} = \sqrt{\frac{1}{2}}\hat{S}_1 - \sqrt{\frac{1}{2}}\hat{S}_2e^{i\varphi_S}, \quad (1)$$

\hat{a} and \hat{b} are experimentally characterized by the subtracting of the photocurrents of the BHD and can be expressed as

$$\begin{aligned} i_a &= i_{a1} - i_{a2} = \hat{a}^+ e^{i\varphi_A} + \hat{a} e^{-i\varphi_A} \\ &= \sqrt{\frac{1}{2}} \left(\hat{S}_1 e^{-i\varphi_A} + \hat{S}_1^+ e^{i\varphi_A} \right) + \sqrt{\frac{1}{2}} \left(\hat{S}_2 e^{i\varphi_S} e^{-i\varphi_A} + \hat{S}_2^+ e^{-i\varphi_S} e^{i\varphi_A} \right), \end{aligned} \quad (2)$$

$$\begin{aligned} i_b &= i_{b1} - i_{b2} = \hat{b}^+ e^{i\varphi_B} + \hat{b} e^{-i\varphi_B} \\ &= \sqrt{\frac{1}{2}} \left(\hat{S}_1 e^{-i\varphi_B} + \hat{S}_1^+ e^{i\varphi_B} \right) - \sqrt{\frac{1}{2}} \left(\hat{S}_2 e^{i\varphi_S} e^{-i\varphi_B} + \hat{S}_2^+ e^{-i\varphi_S} e^{i\varphi_B} \right), \end{aligned} \quad (3)$$

where the relative phase φ_A (or φ_B) between the local oscillator and entangled mode A (or B) determines the variance of the measured quadrature. If $\varphi_A = \varphi_B = 0$ or $\frac{\pi}{2}$, the quadrature photocurrents sum $V(\hat{X}_a + \hat{X}_b)$ of amplitude or difference $V(\hat{Y}_a - \hat{Y}_b)$ of phase correlation can

be deduced as

$$\begin{aligned}
 i_A \pm i_B = & \sqrt{\frac{1}{2}} \left[\left(\hat{S}_1 + \hat{S}_1^+ \right) (\cos \varphi_A \pm \cos \varphi_B) + i \left(\hat{S}_1^+ - \hat{S}_1 \right) (\sin \varphi_A \pm \sin \varphi_B) \right] + \\
 & \sqrt{\frac{1}{2}} \left[\left(\hat{S}_2 + \hat{S}_2^+ \right) (\cos \varphi_A \cos \varphi_S \mp \cos \varphi_B \cos \varphi_S + \sin \varphi_A \sin \varphi_S \mp \sin \varphi_B \sin \varphi_S) \right] + \\
 & \sqrt{\frac{1}{2}} \left[i \left(\hat{S}_2^+ - \hat{S}_2 \right) (\sin \varphi_A \cos \varphi_S \mp \sin \varphi_B \cos \varphi_S - \cos \varphi_A \sin \varphi_S \pm \cos \varphi_B \sin \varphi_S) \right],
 \end{aligned} \quad (4)$$

The correlation variances of the entanglement can be given as the square of $i_A \pm i_B$

$$\begin{aligned}
 V(A \pm B) = & \frac{1}{2} \left[V_{S1}(X) (\cos \varphi_A \pm \cos \varphi_B)^2 + V_{S1}(Y) (\sin \varphi_A \pm \sin \varphi_B)^2 \right] + \\
 & \frac{1}{2} \left[V_{S2}(X) (\cos \varphi_A \cos \varphi_S \mp \cos \varphi_B \cos \varphi_S + \sin \varphi_A \sin \varphi_S \mp \sin \varphi_B \sin \varphi_S)^2 \right] + \\
 & \frac{1}{2} \left[V_{S2}(Y) (\sin \varphi_A \cos \varphi_S \mp \sin \varphi_B \cos \varphi_S - \cos \varphi_A \sin \varphi_S \pm \cos \varphi_B \sin \varphi_S)^2 \right],
 \end{aligned} \quad (5)$$

where $V_{S1}(X) = \hat{X}_{S1}^2 = \left(\hat{S}_1 + \hat{S}_1^+ \right)^2$ (or $V_{S2}(X)$) and $V_{S1}(Y) = \hat{Y}_{S1}^2 = \left[i \left(\hat{S}_1^+ - \hat{S}_1 \right) \right]^2$ (or $V_{S2}(Y)$) are the noise variances of the amplitude and phase quadratures for squeezed mode \hat{S}_1 (or \hat{S}_2), respectively. Apparently, squeezing variances directly determine the maximum entanglement strength, while the rotation of the squeezed angle $\theta_{1,2}$ has a negative function on the quadrature variances [28,29]

$$V_{S1,2}(X) = V_{10,20}(X) \cos^2 \left(\frac{\theta_{1,2}}{2} \right) + V_{10,20}(Y) \sin^2 \left(\frac{\theta_{1,2}}{2} \right), \quad (6)$$

$$V_{S1,2}(Y) = V_{10,20}(Y) \cos^2 \left(\frac{\theta_{1,2}}{2} \right) + V_{10,20}(X) \sin^2 \left(\frac{\theta_{1,2}}{2} \right), \quad (7)$$

The squeezed angle $\theta_{1,2}$ is associated with the relative phase between the signal and pump beams $\Phi_{1,2}$ [28–30]. $\Phi_{1,2} = \pi$ corresponds to the de-amplification of the OPA. Here, $V_{10}(X)$, $V_{10}(Y)$ and $V_{20}(X)$, $V_{20}(Y)$ are the initial variances of the amplitude and phase quadratures of the two squeezed states [28,29,31–33]

$$\begin{aligned}
 V_{10,20}(X/Y) = & \left(1 \mp \frac{4\eta_{1,2} \sqrt{P_{1,2}/P_{th1,2}}}{\left(1 \pm \sqrt{P_{1,2}/P_{th1,2}} \right)^2 + 4(f/\nu_{1,2})^2} \right) \cos^2 \theta_{\text{rms}} \\
 & + \left(1 \pm \frac{4\eta_{1,2} \sqrt{P_{1,2}/P_{th1,2}}}{\left(1 \mp \sqrt{P_{1,2}/P_{th1,2}} \right)^2 + 4(f/\nu_{1,2})^2} \right) \sin^2 \theta_{\text{rms}},
 \end{aligned} \quad (8)$$

Here ν is the full-width at half-maximum (FWHM) linewidth of the OPA, f is the analysis frequency, and η is the total detection efficiency. $P_{1,2}$ is the pump power, and $P_{th1,2}$ is the threshold pump power of the OPA. θ_{rms} is fluctuation in the squeezing angle and is referred to the root-mean-square (rms) of the total phase noise, which makes the amplified noise in orthogonal quadrature couple into the observed squeezed quadrature. Losses and phase noises finally codetermine the measured squeezing level.

Consequently, five phase angles (Φ_1 , Φ_2 , φ_S , φ_A , φ_B) determine the final correlations measured by BHDs, and the upstream phase deviations are also accumulated in the downstream as showing

in Fig. 1(a). To quantify the accumulated phase deviation effect, we redefine the relative phases as $\Phi_{1,2}=\Phi_{10,20}+\Delta\Phi_{1,2}$, $\varphi_S=\varphi_{S0}+\Delta\varphi_S$, and $\varphi_{A,B}=\varphi_{A0,B0}+\Delta\varphi_{A,B}$. As showing in Fig. 1(b), $\Delta\Phi_{1,2}$ results in a rotation of the squeezed angle ($\theta_{1,2}=\theta_{10,20}+\Delta\theta_{1,2}$) during the preparation of squeezed state, meanwhile leads to an increased output power P_{out1} of the OPA (operating on de-amplification), and the power ratio R of P_{out1} to the initial one P_{out0} can be deduced as [34]

$$R = \frac{1 + \frac{P_{1,2}}{P_{th1,2}} + 2 \cos(\Phi_{10,20} + \Delta\Phi_{1,2}) \sqrt{\frac{P_{1,2}}{P_{th1,2}}}}{1 + \frac{P_{1,2}}{P_{th1,2}} + 2 \cos(\Phi_{10,20}) \sqrt{\frac{P_{1,2}}{P_{th1,2}}}}, \quad (9)$$

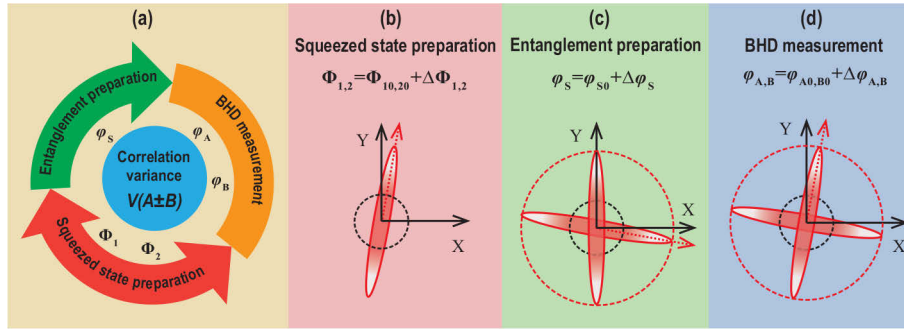


Fig. 1. Building blocks of the relative phase angles and the principle of phase deviation during entanglement generation: relationship of the relative phases for (a) the squeezed state, entangled state preparation and measurement, (b) squeezed state preparation, (c) entanglement preparation, (d) BHD measurement.

In this case, if the error signal for φ_S locking is extracted from the amplitude of the interference of the two squeezed beams, $\Delta\Phi_{1,2}$ induced power variation will lead to a phase deviation to φ_S (Fig. 1(c)), because of the zero point of the error signal deviates from the middle of the interference fringe. Combining the equation of R and the quantitative equation of the interference intensity, φ_S can be modified as

$$\varphi_S = \varphi_{S0} + \Delta\varphi_S = \arccos \frac{I_2^2 - R^2 + 2I_1I_2 \cos \varphi_{S0}}{2I_1R}, \quad (10)$$

If the initial power of the two squeezed beams is normalized to 1 ($I_1=I_2=1$), then φ_S is simplified to $\varphi_S = \arccos \frac{1-R^2}{2R}$. With this methodology, the deviation of φ_S related to $\Delta\Phi_{1,2}$ can be quantitatively demonstrated as describing in Fig. 2(a). For example, a 20 mrad phase deviation of Φ_1 results in a 13 mrad deviation of φ_S , i.e., $\Phi_1 = \pi \pm 0.02$ rad, $\varphi_S = \frac{\pi}{2} + 0.013$ rad. Furthermore, as showing in Fig. 1(d), $\Delta\varphi_{A,B}$ will also introduce a squeezing angle rotation between the measurement base of the BHDs and entanglement quadratures.

We comprehensively illustrate the influence of $\Delta\Phi_{1,2}$, $\Delta\varphi_S$, and $\Delta\varphi_{A,B}$ on entanglement correlations in Fig. 2(b)-(d) by simultaneous equations (5)-(10). Figure 2(b) shows the entanglement correlations noise power individually and independently relating to the deviations of the relative phases. It is clear from the figure that all the deviations of the relative phases excite phase angle rotation and contribute to the noise power growth, but we note that the dominant contributor to the magnitude of the noise power is the phase deviation of φ_S (red line in Fig. 2(b)), while $\Delta\Phi_{1,2}$ will exacerbate this contribution in practical entangled states preparation (blue line in Fig. 2(b)).

Whereafter assuming a precise locking of φ_S as a prerequisite, $\Delta\Phi_{1,2}$ and $\Delta\varphi_{A,B}$ are considered to demonstrate the relation of the relative phase deviation and entanglement noise power. As

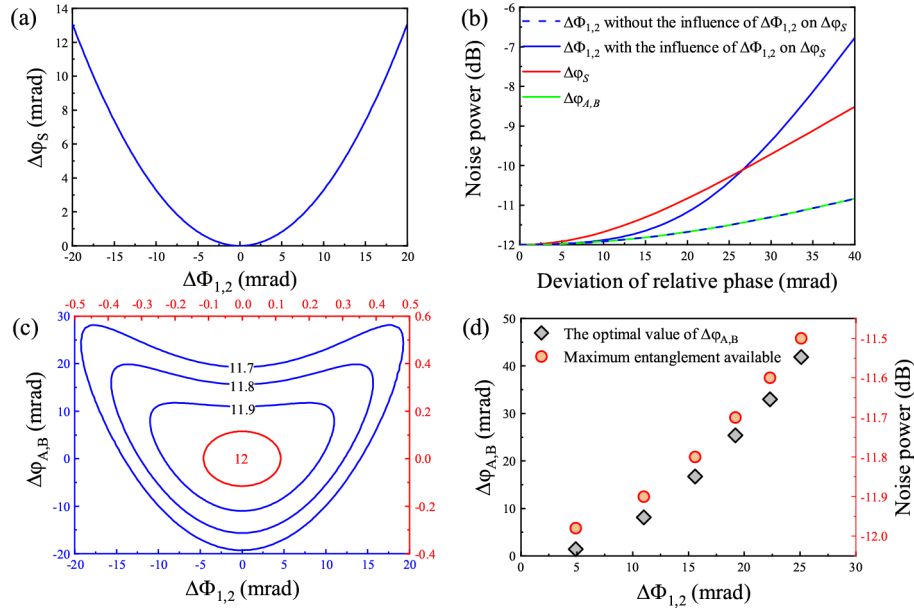


Fig. 2. Demonstration that in relating the phase deviation to entanglement noise power is necessary for high degree entangled states generation. (a) $\Delta\varphi_S$ versus $\Delta\Phi_{1,2}$, (b) entanglement degree versus $\Delta\Phi_{1,2}$ with (blue line) and without (blue dotted line) the influence of $\Delta\Phi_{1,2}$ on $\Delta\varphi_S$, $\Delta\varphi_S$ (red line), $\Delta\varphi_{A,B}$ (green line), (c) $\Delta\varphi_{A,B}$ versus $\Delta\Phi_{1,2}$ for different entanglement degree with the influence of $\Delta\Phi_{1,2}$ on $\Delta\varphi_S$, (d) the optimal value of $\Delta\varphi_{A,B}$ (black prismatic) and maximum entanglement available (red circle) versus $\Delta\Phi_{1,2}$ with the influence of $\Delta\Phi_{1,2}$ on $\Delta\varphi_S$. The squeezing degree used to calculate the entanglement is -12 dB.

showing in Fig. 2(c), the deviation range of the relative phase should be more and more narrow with the degree of entanglement increasing. For example, both $\Delta\Phi_{1,2}$ and $\Delta\varphi_{A,B}$ should be precisely controlled to 0.1 mrad for 12 dB entanglement (red line in Fig. 2(c)), while relax to $+30/-20$ mrad for the 11.7 dB one. From Fig. 2(c), it also can be found an optimum $\Delta\varphi_{A,B}$ for a certain $\Delta\Phi_{1,2}$, and the results are shown in Fig. 2(d). Clearly, with the increasing of $\Delta\Phi_{1,2}$, the available maximum degree of the entanglement gradually decreases. Therefore, $\Delta\Phi_{1,2}$ and $\Delta\varphi_S$ are more harmful for high degree entanglement generation, which should involve stepping up more effort to suppress.

3. Experimental setup and result

The schematic of our experimental setup is illustrated in Fig. 3. The laser source is a continuous-wave single-frequency fiber laser with an output power of 2 W at 1550 nm wavelength (E15, *NKT Photonics*). The mode cleaners (MCs) are employed to ensure the quadrature noises of the fundamental and second harmonic waves meet SNL above 5 MHz [30]. Here one of the 1550 nm MCs is omitted in Fig. 3. The fundamental wave serves as the seed beams of the degenerate OPAs (DOPAs) and local oscillators (LO, 10 mW) of the BHDs. Meanwhile, it is also applied to produce an up-conversion wave of 105 mW by the second harmonic generator (SHG), which is used as the pump laser of the DOPAs. Both of the DOPAs are semi-monolithic double-resonant cavities and their parameters are the same as Ref. [30], in which the pump beams are modulated with 42.5 MHz and used for cavity length sensing and locking. The outputs of the DOPAs are coupled on a 50/50 BS to prepare the entangled beams. The SHG has similar parameters with DOPA, except for a concave mirror with a transmissivity of $12\% \pm 1.5\%$ for 1550 nm and high

transmission for 775 nm. The resonant conditions of the DOPAs and MCs are maintained by Pound-Drever-Hall (PDH) technique [35].

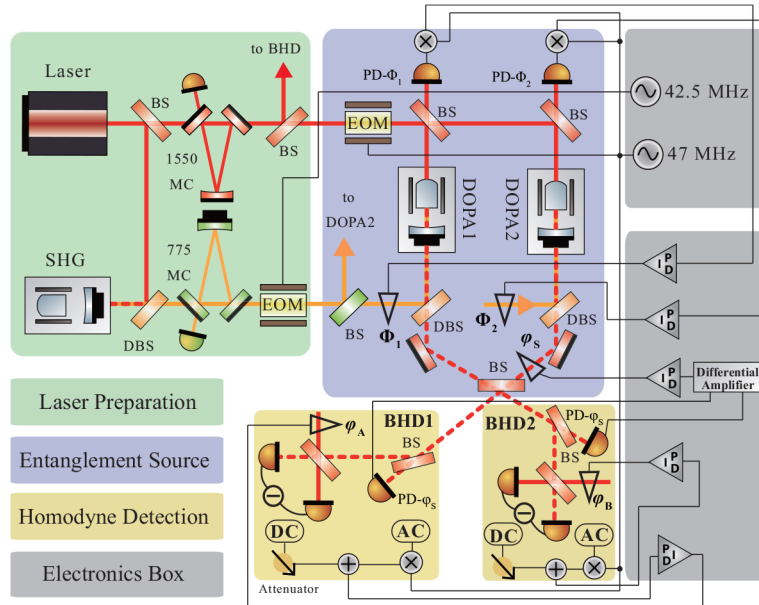


Fig. 3. Schematic of the entangled light source and feedback control loops for relative phase. MC, mode cleaner; SHG, second harmonic generator; DOPA, degenerate optical parametric amplifier; DBS, dichroic beam splitter; BS, beam splitter; EOM, electrooptical modulator; PD, photodetector; BHD, balanced homodyne detector.

The major concern of a robust entangled state in this work is the precise control of the relative phases as stating in section 2. To satisfy the requirement of ultralow phase deviation, we have developed an ultralow RAM control loop in previous researches [27,28,36], and upgrade the phase-locking technologies in this work are summarized in Table 1. The ultralow RAM control loops make sure the stable and precise locking of the cavities and $\Phi_{1,2}$. With this method, the squeezing phase noise could be controlled to 1.4 ± 0.26 mrad in a double-resonant OPA process [30], and the zero-baseline offset of the error signals was reduced to $+70/-50$ ppm, about 1/50 without the ultralow RAM design.

Table 1. Summary of the locking technique of the relative phase. See main text for further discussion.

Phase angle	Brief description	Locking technique
Φ_1 (Φ_2)	π phase in de-amplified status of the DOPAs	PDH via reflection of the DOPAs, 47 MHz [30]
φ_S	$\pi/2$ phase between two squeezed beams	DC locking
φ_A (φ_B)	0 or $\pi/2$ phase of the LO beams	DC-AC joint locking, 47 MHz

Subsequently, 1% powers of the two entangled modes are leaked from the two BSs in the optical paths of the entangled beams. The two dc interference signals read by PD- φ_S are mutually subtracted to produce an error signal centered around zero. This zero-crossing can be directly used to produce an error signal for $\pi/2$ phase locking between the two squeezed beams [14]. It has an advantage to cancel the power fluctuations from the outputs of the DOPAs, and breaks the relevance between R and φ_S .

Finally, to measure the maximum correlations of the entanglement quadratures, i.e., eliminate the deviation of the relative phase $\varphi_{A,B}$ as much as possible, we utilize a DC and AC joint locking technology for arbitrary phase control. The 47 MHz modulated sidebands on the seed beams are demodulated to produce the AC signals $-\sin \theta$ for BHD1 and BHD2, which can be used for 0 phase locking. The demodulated AC signal adds with the DC interference signal $\cos \theta$ (used for $\pi/2$ phase locking) exporting from the same BHD, then forms the final error signal of $\varphi_{A,B}$ as $\varepsilon_{\varphi_{A,B}} = -\sin(\theta - \varphi_{A,B}) = k \cos \theta - \sin \theta$, where $k = \tan \varphi_{A,B}$. Therefore, the error signal of $\varphi_{A,B}$ can be calibrated by modifying the coefficient k , which can be expediently adjusted by the amplitude of the DC part. In our experiment, an attenuator acts as an amplitude adjuster for the DC signal, which is equivalent to modify the value of k . It can be found that $\varphi_{A,B}$ can be locked to $0 \sim \pi/2$ by changing the value of k from 0 to ∞ . This joint locking method is superior to the individual AC or DC locking technology, because it can conveniently calibrate the relative phases to the exact value by adjusting k and promote us to read out the optimum quadrature correlations.

By optimizing the feedback control loops of the relative phases with the above methodologies, an entanglement, with quadrature amplitude and phase correlations of -10.9 ± 0.2 dB and -11.1 ± 0.2 dB at 5 MHz (Agilent N9020A), was directly observed by joint measurements of BHD1 and BHD2. Figure 4 presents the measured results at the pump power of 13.5 mW, and the detailed experimental parameters are also given in Table 3. All traces are normalized to the SNL corresponding to a 10 mW LO. Trace (I) corresponds to the SNL with entangled light blocked. Trace (II) and (III) are the variances of the quadrature amplitude and phase correlations. The electronic noise (Trace (IV)) of the BHD is 21 dB below SNL. Figure 4(a) shows the directly observed quadrature amplitude and phase correlations at 5 MHz with an inseparability criterion of the correlations of $\sqrt{V(\hat{X}_a + \hat{X}_b) V(\hat{Y}_a - \hat{Y}_b)} = 0.079$. By subtracting the contribution of the electronic noise, the amplitude and phase correlations are amended to -11.1 dB and -11.3 dB. Figure 4(b) presents a broadband quantum noise correlation in the frequency range from 5 to 100 MHz. The quadrature amplitude and phase correlations are -2.4 ± 0.2 dB and -2.6 ± 0.2 dB at 100 MHz with an inseparability criterion of the correlations of $\sqrt{V(\hat{X}_a + \hat{X}_b) V(\hat{Y}_a - \hat{Y}_b)} = 0.56$.

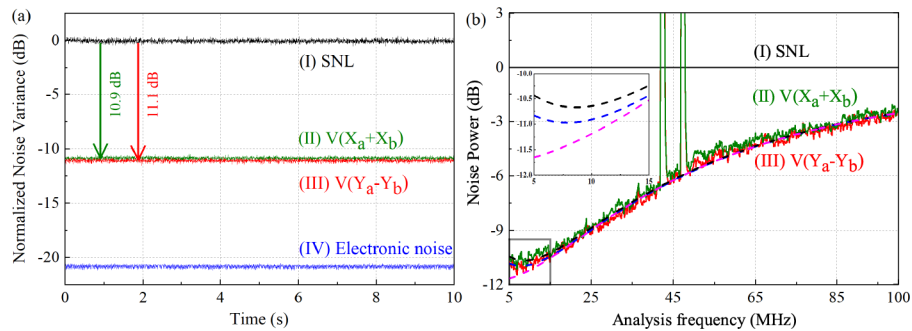


Fig. 4. Variances of the sum $V(\hat{X}_a + \hat{X}_b)$ of the amplitude and difference $V(\hat{Y}_a - \hat{Y}_b)$ of the phase quadratures. (a) Variances at analysis frequency of 5 MHz and (b) between 5 MHz and 100 MHz with a resolution bandwidth (RBW) of 300 kHz and a video bandwidth (VBW) of 200 Hz.

The data in Fig. 4(b) are fitted with the model of Eq. (5) (the black and blue dotted lines) [37], and it gains a total optical loss of $6.5\% \pm 0.14\%$, and a phase noise of 9.7 ± 0.32 or 11.1 ± 0.36 mrad for phase or amplitude quadrature, respectively. Table 2 lists all known sources of loss and phase noise in the entanglement preparation [31–33,38]. With one of the OPAs, the total phase noise for one-mode squeezing had been confirmed to be 1.4 ± 0.26 mrad [30]. For phase

noise measurement in DC-AC joint locking of the BHDs, the seed beam exits the OPA with the temperature of PPKTP far away from the phase matching condition, and the phase noise was determined to be 1.7 ± 0.2 mrad. The phase noise between the two squeezed beams limits the noise to be 9.9 ± 0.3 mrad, which is attributed to the lower signal-to-noise ratio for weak signal extraction in the photodetector. Finally, the total loss and phase noise codetermine the measured squeezing level. The impact of phase noise becomes more acute as the losses are reduced (Fig. 1 of [32]). Compared with the results of the fitted curves in Fig. 4(b), it concludes that the maximum squeezing can reach to -11.6 dB with 0 phase noise (the pink dotted line in Fig. 4(b)). Therefore, loss is the dominating limitation for the enhancement of the squeezing level, and should be furtherly reduced.

Table 2. Loss and Phase Noise Budget for our entangled light source.

Source of Loss	Value (%)
OPO escape efficiency	98 ± 0.47
Propagation efficiency	98 ± 0.2
Three 99.7% interference visibility	99.4 ± 0.2
Photodiode quantum efficiency	99 ± 0.2
Total efficiency	93.5 ± 0.14
Source of Phase Noise	Value (mrad)
MC length noise	0.1 ± 0.1
SHG length noise	0.2 ± 0.1
OPO detuning noise	0.23 ± 0.1
Noise for π phase in de-amplified status of the DOPAs	0.52 ± 0.2
Noise for $\pi/2$ phase between the two squeezed beams	9.9 ± 0.3
Noise for 0 or $\pi/2$ phase of the LO beams	1.7 ± 0.2
Total phase noise	9.7 ± 0.32 (phase) 11.1 ± 0.36 (amplitude)

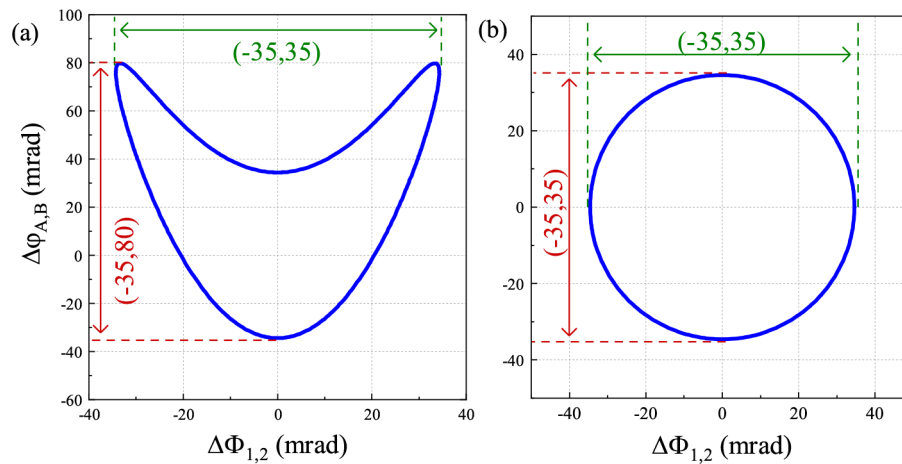


Fig. 5. Simulated results of the phase deviation $\Delta\Phi_{1,2}$ and $\Delta\varphi_{A,B}$ of the -11 dB entanglement based on the experimental parameters in Table 3 and theoretical models in section 2. Extracting the error signal of φ_S from (a) one of the entangled modes or (b) the difference of the two entangled modes.

With the results in Fig. 4(a) and Table 3, the phase-locking accuracy is calculated as showing in Fig. 5. When extracts the error signal of φ_S from one of the entangled modes, our phase-locking technology controls $\Delta\varphi_{A,B}$ in the range of -35 to 80 mrad (Fig. 5(a)). When the difference of the two entangled modes is applied to lock the φ_S , it can be found that $\Delta\varphi_{A,B}$ is reduced to the range of -35 to 35 mrad (Fig. 5(b)), due to the elimination of the influence of $\Delta\Phi_{1,2}$ to $\Delta\varphi_S$. In the two cases, $\Delta\Phi_{1,2}$ always keeps in the locking range of -35 to 35 mrad. Therefore, the precise control of the relative phases in our entanglement light source is established.

Table 3. The experimental parameters used for the calculation of Fig. 5.

Parameter	$\nu_{1,2}$ MHz	$f_{1,2}$ MHz	$\eta_{1,2}$ %	$P_{1,2}$ mW	$P_{th,1,2}$ mW	φ_S rad	$V_{10,20}(X)$ dB	$V(\hat{X}_a + \hat{X}_b)$ dB	$V(\hat{Y}_a - \hat{Y}_b)$ dB
Value	110	5	95	13.5	16.6	$\frac{\pi}{2}$	-12.3	-10.9	-11.1

4. Conclusion

The experimental and theoretical analyses of the influence of relative phases for enhancing the correlations of entanglement were first demonstrated. The experimental results well agree with the theoretical ones, that take into account the internal relations of the relative phases (Φ_1 , Φ_2 , φ_S , φ_A and φ_B) during the preparation, transmission, and detection of entangled states. To ensure a high degree of entanglement, three precisely phase-locking technologies are established: ultralow RAM control loops for the lengths and relative phases of the DOPAs, difference DC locking for the relative phase between the two squeezed beams, and DC-AC joint locking for the relative phases in BHDs. The phase-locking loops ensure the total phase noise to be $9.7 \pm 0.32 / 11.1 \pm 0.36$ mrad. Attributing to the accuracy control of the relative phases to the range of -35 to 35 mrad, the amplitude and phase correlations of the entangled state are enhanced to -11.1 and -11.3 dB, and also owns a broadband squeezing with bandwidth more than 100 MHz. We envision that the valuable entanglement resource will widen the applications of quantum information networks, quantum computation, quantum communication, and quantum precision measurement.

Funding. National Natural Science Foundation of China (62027821, 11654002, 11874250, 11804207, 11804206, 62035015); National Key Research and Development Program of China (2020YFC2200402); Key Research and Development Projects of Shanxi Province (201903D111001); Program for Outstanding Innovative Teams of Higher Learning Institutions of Shanxi; Program for Sanjin Scholar of Shanxi Province; Fund for Shanxi “1331 Project” Key Subjects Construction.

Disclosures. The authors declare no conflicts of interest.

Data availability. Data underlying the results presented in this paper are not publicly available at this time but may be obtained from the authors upon reasonable request.

References

- U. L. Andersen, J. S. Neergaard-Nielsen, P. van Loock, and A. Furusawa, “Hybrid discrete-and continuous-variable quantum information,” *Nat. Phys.* **11**(9), 713–719 (2015).
- W. McCutcheon, A. Pappa, B. A. Bell, A. McMillan, A. Chailloux, T. Lawson, M. Mafu, D. Markham, E. Diamanti, I. Kerenidis, J. G. Rarity, and M. S. Tame, “Experimental verification of multipartite entanglement in quantum networks,” *Nat. Commun.* **7**(1), 13251 (2016).
- B. Zhang and Q. Zhuang, “Entanglement formation in continuous-variable random quantum networks,” *npj Quantum Inf.* **7**(1), 33 (2021).
- M. H. Wang, Y. Xiang, H. J. Kang, D. M. Han, Y. Liu, Q. Y. He, Q. H. Gong, X. L. Su, and K. C. Peng, “Deterministic distribution of multipartite entanglement and steering in a quantum network by separable states,” *Phys. Rev. Lett.* **125**(26), 260506 (2020).
- S. Armstrong, M. Wang, R. Y. Teh, Q. Gong, Q. He, J. Janousek, H. A. Bachor, M. D. Reid, and P. K. Lam, “Multipartite Einstein–Podolsky–Rosen steering and genuine tripartite entanglement with optical networks,” *Nat. Phys.* **11**(2), 167–172 (2015).
- N. C. Menicucci, P. van Loock, M. Gu, C. Weedbrook, T. C. Ralph, and M. A. Nielsen, “Universal quantum computation with continuous-variable cluster states,” *Phys. Rev. Lett.* **97**(11), 110501 (2006).
- X. L. Su, S. H. Hao, X. W. Deng, L. Y. Ma, M. H. Wang, X. J. Jia, C. D. Xie, and K. C. Peng, “Gate sequence for continuous variable one-way quantum computation,” *Nat. Commun.* **4**(1), 2828 (2013).

8. L. S. Madsen, V. C. Usenko, M. Lassen, R. Filip, and U. L. Andersen, "Continuous variable quantum key distribution with modulated entangled states," *Nat. Commun.* **3**(1), 1083 (2012).
9. C. Weedbrook, "Continuous-variable quantum key distribution with entanglement in the middle," *Phys. Rev. A* **87**(2), 022308 (2013).
10. S. Pirandola, J. Eisert, C. Weedbrook, A. Furusawa, and S. L. Braunstein, "Advances in quantum teleportation," *Nat. Photonics* **9**(10), 641–652 (2015).
11. M. R. Huo, J. L. Qin, J. L. Cheng, Z. H. Yan, Z. Z. Qin, X. L. Su, X. J. Jia, C. D. Xie, and K. C. Peng, "Deterministic quantum teleportation through fiber channels," *Sci. Adv.* **4**(10), eaas9401 (2018).
12. S. P. Shi, L. Tian, Y. J. Wang, Y. H. Zheng, C. D. Xie, and K. C. Peng, "Demonstration of channel multiplexing quantum communication exploiting entangled sideband modes," *Phys. Rev. Lett.* **125**(7), 070502 (2020).
13. S. Takeda, M. Fuwa, P. van Loock, and A. Furusawa, "Entanglement swapping between discrete and continuous variables," *Phys. Rev. Lett.* **114**(10), 100501 (2015).
14. T. C. Zhang, K. W. Goh, C. W. Chou, P. Lodahl, and H. J. Kimble, "Quantum teleportation of light beams," *Phys. Rev. A* **67**(3), 033802 (2003).
15. W. Wasilewski, K. Jensen, H. Krauter, J. J. Renema, M. V. Balabas, and E. S. Polzik, "Quantum Noise Limited and Entanglement-Assisted Magnetometry," *Phys. Rev. Lett.* **104**(13), 133601 (2010).
16. S. Steinlechner, J. Bauchrowitz, M. Meinders, H. Müller-Ebhardt, K. Danzmann, and R. Schnabel, "Quantum-dense metrology," *Nat. Photonics* **7**(8), 626–630 (2013).
17. Y. Ma, H. Miao, B. H. Pang, M. Evans, C. Zhao, J. Harms, R. Schnabel, and Y. Chen, "Proposal for gravitational-wave detection beyond the standard quantum limit through EPR entanglement," *Nat. Phys.* **13**(8), 776–780 (2017).
18. J. Südbeck, S. Steinlechner, M. Korobko, and R. Schnabel, "Demonstration of interferometer enhancement through Einstein–Podolsky–Rosen entanglement," *Nat. Photonics* **14**(4), 240–244 (2020).
19. M. J. Yap, P. Altin, T. G. McRae, B. J. J. Slagmolen, R. L. Ward, and D. E. McClelland, "Generation and control of frequency-dependent squeezing via Einstein–Podolsky–Rosen entanglement," *Nat. Photonics* **14**(4), 223–226 (2020).
20. S. Steinlechner, J. Bauchrowitz, T. Eberle, and R. Schnabel, "Strong Einstein–Podolsky–Rosen steering with unconditional entangled states," *Phys. Rev. A* **87**(2), 022104 (2013).
21. Y. J. Wang, W. H. Zhang, R. X. Li, L. Tian, and Y. H. Zheng, "Generation of -10.7 dB unbiased entangled states of light," *Appl. Phys. Lett.* **118**(13), 134001 (2021).
22. T. Eberle, V. Händchen, and R. Schnabel, "Stable control of 10 dB two-mode squeezed vacuum states of light," *Opt. Express* **21**(9), 11546–11553 (2013).
23. W. P. Bowen, P. K. Lam, and T. C. Ralph, "Biased EPR entanglement and its application to teleportation," *J. Mod. Opt.* **50**(5), 801–813 (2003).
24. A. Khalaidovski, H. Vahlbruch, N. Lastzka, C. Gräf, K. Danzmann, H. Grote, and R. Schnabel, "Long-term stable squeezed vacuum state of light for gravitational wave detectors," *Classical Quantum Gravity* **29**(7), 075001 (2012).
25. J. Arnbak, C. S. Jacobsen, R. B. Andrade, X. Guo, J. S. Neergaard-Nielsen, U. L. Andersen, and T. Gehring, "Compact, low-threshold squeezed light source," *Opt. Express* **27**(26), 37877–37885 (2019).
26. Z. X. Li, Y. H. Tian, Y. J. Wang, W. G. Ma, and Y. H. Zheng, "Residual amplitude modulation and its mitigation in wedged electro-optic modulator," *Opt. Express* **27**(5), 7064–7071 (2019).
27. Z. X. Li, W. G. Ma, W. H. Yang, Y. J. Wang, and Y. H. Zheng, "Reduction of zero baseline drift of the Pound–Drever–Hall error signal with a wedged electro-optical crystal for squeezed state generation," *Opt. Lett.* **41**(14), 3331–3334 (2016).
28. W. H. Yang, S. P. Shi, Y. J. Wang, W. G. Ma, Y. H. Zheng, and K. C. Peng, "Detection of stably bright squeezed light with the quantum noise reduction of 12.6 dB by mutually compensating the phase fluctuations," *Opt. Lett.* **42**(21), 4553–4556 (2017).
29. H. Vahlbruch, M. Mehmet, K. Danzmann, and R. Schnabel, "Detection of 15 dB Squeezed States of Light and their Application for the Absolute Calibration of Photoelectric Quantum Efficiency," *Phys. Rev. Lett.* **117**(11), 110801 (2016).
30. W. H. Zhang, J. R. Wang, Y. H. Zheng, Y. J. Wang, and K. C. Peng, "Optimization of the squeezing factor by temperature-dependent phase shift compensation in a doubly resonant optical parametric oscillator," *Appl. Phys. Lett.* **115**(17), 171103 (2019).
31. E. Oelker, G. Mansell, M. Tse, J. Miller, F. Matichard, L. Barsotti, P. Fritschel, D. E. McClelland, M. Evans, and N. Mavalvala, "Ultra-low phase noise squeezed vacuum source for gravitational wave detectors," *Optica* **3**(7), 682–685 (2016).
32. S. Dwyer, L. Barsotti, S. S. Y. Chua, M. Evans, M. Factourovich, D. Gustafson, T. Isogai, K. Kawabe, A. Khalaidovski, P. K. Lam, M. Landry, N. Mavalvala, D. E. McClelland, G. D. Meadors, C. M. Mow-Lowry, R. Schnabel, R. M. S. Schofield, N. Smith-Lefebvre, M. Stefszky, C. Vorvick, and D. Sigg, "Squeezed quadrature fluctuations in a gravitational wave detector using squeezed light," *Opt. Express* **21**(16), 19047–19060 (2013).
33. E. Oelker, L. Barsotti, S. Dwyer, D. Sigg, and N. Mavalvala, "Squeezed light for advanced gravitational wave detectors and beyond," *Opt. Express* **22**(17), 21106–21121 (2014).
34. K. McKenzie, M. B. Gray, P. K. Lam, and D. E. McClelland, "Nonlinear phase matching locking via optical readout," *Opt. Express* **14**(23), 11256–11264 (2006).
35. E. D. Black, "An introduction to Pound–Drever–Hall laser frequency stabilization," *Am. J. Phys.* **69**(1), 79–87 (2001).

36. C. Y. Chen, Z. X. Li, X. L. Jin, and Y. H. Zheng, "Resonant photodetector for cavity-and phase-locking of squeezed state generation," *Rev. Sci. Instrum.* **87**(10), 103114 (2016).
37. M. Mehmet, S. Ast, T. Eberle, S. Steinlechner, H. Vahlbruch, and R. Schnabel, "Squeezed light at 1550nm with a quantum noise reduction of 12.3 dB," *Opt. Express* **19**(25), 25763–25772 (2011).
38. N. Kijbunchoo, T. McRae, D. Sigg, S. E. Dwyer, H. Yu, L. McCuller, L. Barsotti, C. D. Blair, A. Effler, M. Evans, A. Fernandez-Galiana, V. V. Frolov, F. Matichard, N. Mavalvala, A. Mullavey, B. J. J. Slagmolen, M. Tse, C. Whittle, and D. E. McClelland, "Low phase noise squeezed vacuum for future generation gravitational wave detectors," *Classical Quantum Gravity* **37**(18), 185014 (2020).